

Magnetic dipolar interaction in an atomic Bose Einstein condensate interferometer

M. Fattori,^{1,2} G. Roati,^{1,3} B. Deissler,¹ C. D'Errico,^{1,3} M. Zaccanti,¹
M. Jona-Lasinio,¹ L. Santos,⁴ M. Inguscio,^{1,3} and G. Modugno^{1,3}

¹*LENS and Dipartimento di Fisica, Università di Firenze, and INFN-CNR
Via Nello Carrara 1, 50019 Sesto Fiorentino, Italy*

²*Museo Storico della Fisica e Centro Studi e Ricerche 'Enrico Fermi', Compendio del Viminale, 00184 Roma, Italy*

³*INFN, Sezione di Firenze, Via Sansone 1, 50019 Sesto Fiorentino, Italy*

⁴*Institut für Theoretische Physik, Leibniz Universität, D-30167 Hannover, Germany*

We study the role played by the magnetic dipole interaction in an atomic interferometer based on an alkali Bose-Einstein condensate with tunable scattering length. We tune the s-wave interaction to zero using a magnetic Feshbach resonance and measure the decoherence of the interferometer induced by the weak residual interaction between the magnetic dipoles of the atoms. We prove that with a proper choice of the scattering length it is possible to compensate for the dipolar interaction and extend the coherence time of the interferometer. We put in evidence the anisotropic character of the dipolar interaction by working with two different experimental configurations for which the minima of decoherence are achieved for a positive and a negative value of the scattering length, respectively. Our results are supported by a theoretical model we develop. This model indicates that the magnetic dipole interaction should not represent a serious source of decoherence in atom interferometers based on Bose-Einstein condensates.

PACS numbers: 03.75.Dg, 03.75.Lm, 03.75.Gg

Atom-atom interactions represent a fundamental limit to the performance of atomic Bose Einstein condensate (BEC) interferometers [1, 2, 3, 4]. Atomic collisions lead to density-dependent shifts in the interferometric signal, severely compromising its visibility. In two recent works [5, 6], the possibility to strongly reduce the interaction-induced decoherence in a trapped BEC interferometer has been demonstrated by tuning the s-wave scattering length a almost to zero via a magnetic Feshbach resonance. The tunability of a by magnetic means is possible for atoms with a non-vanishing magnetic dipole moment. Therefore, once the s-wave contact interaction is canceled by applying a proper external magnetic field, the magnetic dipole-dipole interaction (MDI) between the atoms remains as a possible source of decoherence for the interferometer. This aspect has been pointed out in [5, 6], but both a theoretical analysis and an experimental study of the problem are still missing. The MDI generally does not play a role in experiments with ultra-cold quantum degenerate alkali atoms, where the small magnetic dipole moment μ is on the order of the Bohr magneton μ_B and leads to a dipolar interaction energy $E_d < 0.01 \cdot E_s$, with E_s the s-wave contact interaction energy. So far, studies of the MDI in an ultra-cold gas have been possible mainly with Cr atoms [7], characterized by a large magnetic dipole moment $\mu = 6\mu_B$ that leads to interaction energies E_d 36 times larger than for alkali atoms. Evidence of MDI in a spinorial alkali BEC has been only recently reported in [8].

In this Letter we study the role played by the MDI in an interferometer where a BEC with weak tunable contact interaction is implemented [5]. We get evidence of the effect of dipolar interaction on the dephasing of the interferometric signal. The MDI is anisotropic and therefore the sign of its contribution to the interaction energy

depends on the geometry of the system. We study in particular two different geometries for which the minimum of decoherence occurs for two different values of the contact interaction, one positive and the other negative. We develop a model that confirms that the minimum of the decoherence is obtained when the contact interaction partially compensates the MDI. The model indicates that the unavoidable MDI should not represent a seriously limiting source of decoherence in BEC-based atom interferometers.

For our studies we implement a Bloch oscillation interferometer [9, 10]. A trapped BEC of ^{39}K atoms [11] is loaded in a deep 1D optical lattice (OL) and an external force F_{ext} along the lattice drives Bloch oscillations. We work with atoms in the absolute ground state $|F = 1, M_F = 1\rangle$ where the magnetic dipole moment $\vec{\mu}$ is parallel to the external magnetic field \vec{B} that is applied to access Feshbach resonances. We can align the OL either along or orthogonal to \vec{B} . Changing $|\vec{B}|$ around 350 G it is possible to finely tune a around a zero crossing [11, 12]. The scattering length can be controlled down to the level of $0.06 a_0$, where the MDI described by the two body potential

$$V_d(\vec{r}) = -\frac{\mu_0 |\vec{\mu}|^2}{4\pi} \left(\frac{3(\hat{\mu} \cdot \hat{r})^2 - 1}{r^3} \right) \quad (1)$$

comes into play. In Eq. (1) $\hat{\mu} = \vec{\mu}/|\vec{\mu}|$ and $r = |\vec{r}|$ is the distance between the two interacting dipoles. Note that the effective dipole moment of ^{39}K atoms at 350G is $\mu = 0.95 \mu_B$ [14]. Due to a quasi 2D geometry of the optical potential in each lattice site, the on-site MDI depends on the orientation of $|\vec{\mu}|$ with respect to the OL. When the dipoles are parallel to the OL (see Fig. 1a)), their mutual interaction within each site is mainly repulsive. A weaker but not negligible attractive contribution comes from dis-

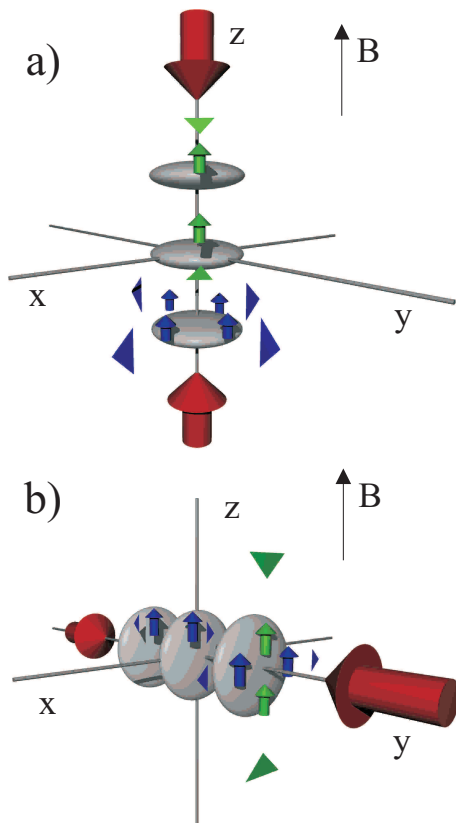


FIG. 1: (Color online) Schematic representation of the character of the magnetic dipolar interaction in the two different experimental configurations. a) For dipoles parallel to the lattice direction, the on-site MDI is repulsive, while the weaker inter-site MDI is attractive. b) For dipoles orthogonal to the lattice direction, the on-site MDI is attractive, while the inter-site MDI is repulsive.

tant sites due to the long range character of the MDI. The non-uniform population over the OL leads to a non homogeneous positive mean field shift causing dephasing of the Bloch oscillations [5, 13]. A proper negative value of a reduces and flattens the interaction mean field shift, increasing the coherence time of the interferometer. In the other configuration, for dipoles orthogonal to the OL (see Fig. 1b), the on site MDI is mainly attractive, the inter sites MDI is slightly repulsive and a proper positive value of a minimizes the decoherence.

In a Bloch oscillation interferometer decoherence manifests itself in a linear increase of the square root of the variance of the atomic momentum distribution as a function of the Bloch oscillations time t_{osc} . It is possible to determine a rate of decoherence from a single measurement of the normalized momentum variance taken at large t_{osc} [5]. Experimentally we measure the momentum distribution by releasing the BEC from the OL and by performing absorption imaging of the atomic density after an expansion of 12 ms.

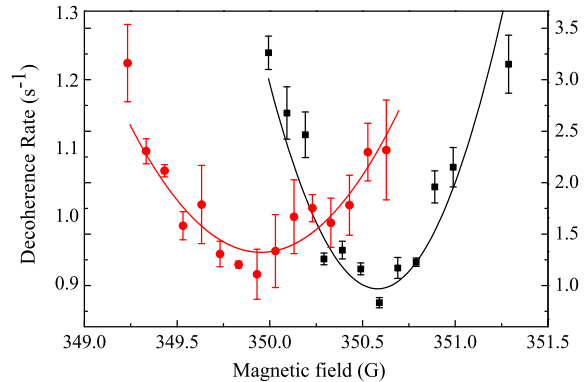


FIG. 2: (Color online) Decoherence rate of the interferometer as a function of the external magnetic field applied during Bloch oscillations for a lattice parallel (circles, left vertical scale) and orthogonal (squares, right vertical scale) to \vec{B} .

The experimental parameters chosen for the measurement of the decoherence rate in the two configurations are listed below. For the OL $\parallel \vec{B}$, we implement a BEC of 4×10^4 atoms initially trapped in a harmonic trap with $(\nu_x, \nu_y, \nu_z) = (76, 44, 43)$ Hz. Before starting Bloch oscillations a is adiabatically tuned to $3 a_0$. The OL has $\nu_x = \nu_y = 44$ Hz and a depth sE_r , where $s = 6$, $E_r = \hbar^2 k_L^2 / 2m$ is the recoil energy, $k_L = 2\pi/\lambda$ is the laser wavevector ($\lambda = 1032$ nm) and m is the atomic mass. In this configuration F_{ext} is the gravitational force. Right after the start of Bloch oscillations, triggered by the switching off of the harmonic trap, a is tuned to a final value around the zero-crossing by tuning the magnetic field. The minimum of decoherence is found at $B_{\perp} = (349.94 \pm 0.02 \pm 0.1)$ G (Fig. 2, circles) (the first uncertainty is statistical, the second one is systematic and comes from the uncertainty in the calibration of the external magnetic field). For the OL $\perp \vec{B}$, Bloch oscillations are driven by a spurious magnetic field gradient generated by the Feshbach coils and the resultant force on the atoms is six times smaller than gravity. For this measurement we use initial trapping frequencies of (99, 45, 109) Hz, a radial lattice confinement $\nu_x = \nu_z = 99$ Hz, $t_{osc} = 300$ ms, $\lambda = 1064$ nm and an average atom number of 2.5×10^4 . Results are shown in Fig. 2 (squares). The minimum of decoherence occurs for a different value of $|\vec{B}|$, i.e. $B_{\parallel} = (350.59 \pm 0.02 \pm 0.1)$ G. Our knowledge of the zero-crossing location ($B_{zc} = 350.4 \pm 0.4$ G) is based on Feshbach spectroscopy analysis [12]. Despite this relatively large uncertainty, one notes that the two minima of decoherence sit on the left and on the right of 350.4 G respectively, in accordance with the qualitative explanation presented above.

For a more quantitative analysis of our findings we have developed a simple theoretical model to describe Bloch oscillations in the presence of the MDI and a weak contact interaction. At sufficiently low interaction strength

our system can be described by a non-local non-linear Schrödinger equation (NLSE) of the form

$$i\hbar \frac{\partial}{\partial t} \Psi(\vec{r}, t) = \left[-\frac{\hbar^2}{2m} \nabla^2 + V_L(z) + V_{\perp}(\rho) - F_{ext}z + \right. \\ \left. + g|\Psi(\vec{r}, t)|^2 + \int d\vec{r}' V_d(\vec{r} - \vec{r}') |\Psi(\vec{r}', t)|^2 \right] \Psi(\vec{r}, t) \quad (2)$$

where $V_L(z) = sE_r \sin^2(k_L z)$ is the lattice potential, $V_{\perp}(\rho) = m\omega_{\perp}^2 \rho^2/2$ describes the transversal harmonic trapping confinement and $g = 4\pi\hbar^2 a/m$. In order to study the two experimental configurations, we fix for simplicity the direction of the lattice along \hat{z} and change the orientation $\hat{\mu}$ of the dipoles. When the lattice depth is sufficiently large, we can implement a tight-binding model. In particular we consider situations where the total interaction energy is much smaller than sE_r and $\hbar\omega_{\perp}$. Therefore we write $\Psi(\vec{r}, t) = \sqrt{N}\phi(\rho) \sum_j \psi_j(t)w(z - z_j)$, where $\phi(\rho) = e^{-\rho^2/2l_{\perp}^2}/\sqrt{\pi}l_{\perp}$ is the transversal ground state, with $l_{\perp} = \sqrt{\hbar/m\omega_{\perp}}$, and $w(z - z_j)$ is the Wannier function associated with the lowest energy band at the j th lattice site located at bj , $b = \pi/k_L$ being the lattice step. For sufficiently deep lattices the Wannier functions are well represented by Gaussians of the form $w(z) = e^{-z^2/2l^2}/\pi^{1/4}\sqrt{l}$, with $b/l = \pi s^{1/4}$. Plugging the tight binding ansatz for $\Psi(\vec{r}, t)$ into eq. (2) and integrating out the spatial coordinates we obtain the discrete NLSE

$$i\hbar \frac{\partial}{\partial t} \psi_j = -J(\psi_{j+1} + \psi_{j-1}) + \Delta j \psi_j + NU^c(a)|\psi_j|^2 \psi_j + \\ + NU_{j,j}^{dd} |\psi_j|^2 \psi_j + N \sum_{\delta \neq 0} U_{j,j+\delta}^{dd} |\psi_{j+\delta}|^2 \psi_j \quad (3)$$

where the five terms on the right are consecutively the tunneling energy, the potential energy due to the external force, the on-site contact interaction term, the on-site MDI term and the inter-site MDI term. In particular $J = \frac{4}{\sqrt{\pi}} s^{3/4} e^{-2\sqrt{s}} E_r$, $\Delta = -F_{ext}b$,

$$U^c(a) = \frac{4\pi\hbar^2}{m} \frac{a}{(2\pi)^{3/2} l_{\perp}^2 l} \quad (4)$$

$$U_{j,j}^{dd} = \xi \frac{\mu_0 \mu^2}{4\pi} \frac{1}{l_{\perp}^3 c^3} \sqrt{\frac{2}{\pi}} \left[\frac{c(3 - c^2)}{3\sqrt{1 - c^2}} - \arcsin(c) \right] \quad (5)$$

where $c = \sqrt{1 - l^2/l_{\perp}^2}$ and where $\xi = (3(\hat{\mu} \cdot \hat{z})^2 - 1)/2$ is a geometric factor taking into account the orientation of the dipoles $\hat{\mu}$ with respect to the lattice direction \hat{z} , and

$$U_{j,j+\delta}^{dd} = \xi \frac{\mu_0 \mu^2}{4\pi} \frac{1}{3l_{\perp}^3} \sqrt{\frac{2}{\pi}} F\left(c, \frac{\delta b}{l_{\perp}}\right) \quad (6)$$

where

$$F(u, v) = \int_0^1 ds \frac{3s^2 - 1}{(1 - u^2 s^2)^{3/2}} \left(1 - \frac{v^2 s^2}{1 - u^2 s^2} \right) e^{-\frac{v^2 s^2}{2(1 - u^2 s^2)}} \quad (7)$$

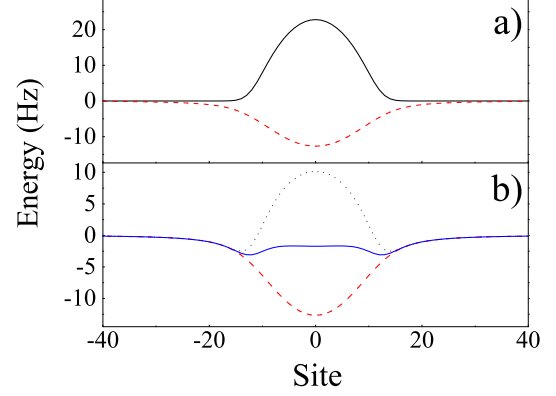


FIG. 3: (Color online) a) On-site dipolar interaction energy (solid line) and inter-site dipolar interaction energy (dashed line) as a function of the lattice site j for the OL $\parallel \vec{B}$ configuration. b) Total interaction energy for $a = 0$ (dotted), $a = -0.52 a_0$ (dashed), i.e. the value that cancels the on-site MDI and for $a = -0.32 a_0$ (solid), i.e. the value that minimizes the decoherence.

Note that Eq.(5) can be obtained by setting $\delta = 0$ in Eq. (6).

The on-site dipole-dipole interaction energy may be re-absorbed in the contact term by defining an effective scattering length a_{eff} such that $U^c(a) + U_{j,j}^{dd} = U^c(a_{eff})$. As a consequence, the on-site interaction energy does not vanish at $a = 0$, but at a finite value \bar{a} such that $a_{eff} = 0$. By equating the contact and on-site dipole-dipole interaction energy we obtain

$$\bar{a} = -\xi \frac{\mu_0 \mu^2}{4\pi} \frac{m}{\hbar^2} \frac{\sqrt{1 - c^2}}{c^3} \left[\frac{c(3 - c^2)}{3\sqrt{1 - c^2}} - \arcsin(c) \right] \quad (8)$$

In the case of ^{39}K we have $m\mu_0\mu^2/(4\pi\hbar^2) = 0.85 a_0$. Using the parameters of our experimental setup we obtain $\bar{a} = -0.52 a_0$ for OL $\parallel \vec{B}$ ($\xi = 1$) and $\bar{a} = 0.24 a_0$ for OL $\perp \vec{B}$ ($\xi = -1/2$). It is then clear that, if we neglect the inter-site MDI, the minima of decoherence for the two lattice configurations would be separated by $(0.24 - (-0.52))a_0 = 0.76 a_0$. To compare theoretical predictions with the experiment we need only to know the $a(|\vec{B}|)$ dependence around the zero crossing, which is known at the percent level. This is $a(|\vec{B}|) = a_{bg} \cdot (|\vec{B}| - B_{zc})/\Delta$, where a_{bg} is the background scattering length of K and Δ the width of the Feshbach resonance we employ [5]. Using the measured values given above, we can calculate $(B_{\parallel} - B_{\perp}) \cdot a_{bg}/\Delta$ and find $(0.36 \pm 0.1)a_0$, clearly not in agreement with the prediction above that takes into account only the on-site MDI. Solving the complete Eq. (3) we find instead that the contribution of the inter-site dipolar coupling is definitely not negligible, and the minima of decoherence are achieved for $\bar{a} = -0.32 a_0$ and $\bar{a} = 0.11 a_0$ for the OL $\parallel \vec{B}$ and the OL $\perp \vec{B}$ respectively, with a consequent separation of $0.43 a_0$. The agreement

with the experiment is now much better, showing the necessity of including the inter-site MDI in the model.

To get a deeper insight into the role played by the long-range character of the dipolar interaction, we plot in Fig. 3a the values of the on-site MDI $N U_{j,j}^{dd} |\psi_j|^2$ and the values of the inter-sites MDI $N \sum_{\delta \neq 0} U_{j,j+\delta}^{dd} |\psi_{j+\delta}|^2$ for the configuration $\text{OL} \parallel \vec{B}$. The inter-site MDI is attractive, in agreement with the qualitative analysis of Eq.1 above, and of the same order of magnitude as the on-site MDI. In Fig. 3 b) we plot the total interaction energy for three cases: $a = 0$, where the residual energy is the total MDI energy; $a = \bar{a} = -0.52 a_0$, where the on-site MDI is perfectly canceled, and the residual energy is due to the inter-sites MDI; $a = -0.32 a_0$, i.e. the value that minimizes the decoherence. Note how a perfect cancelation of the interaction energy is not possible due to the different profiles of the curves in Fig. 3 a), and that the minimum of the decoherence is achieved not when the total interaction energy is averaged to zero, but when its variance is minimized. The partial compensation of the dipolar interaction with the contact interaction allows a reduction of the decoherence rate of our alkali-based interferometer. The model predicts a decoherence rate of 1 Hz for $a=0$ and a residual rate of 0.05 Hz on the minima due to the uncompensated dipolar interaction. Unfortunately we cannot test this prediction because technical noise in our apparatus is presently one order of magnitude larger than this. We plan to study this fundamental limit to the interferometer's coherence with an optimized apparatus

in the near future. A higher sensitivity to interaction-induced decoherence would also allow the verification of the presence of second order effects that cannot be taken into account by our simple model such as dipolar-induced dynamical instabilities [15, 16]. Note that our model predicts the possibility of completely canceling the dipolar interaction by choosing a "magic angle" $\theta = 54.7^\circ$ between the dipoles and the lattice axis for which $\xi = 0$ [17]. A comparison of the differential measurement we have performed with the theoretical prediction can also be used to determine with better accuracy the magnetic-field position of the zero-crossing as $B_{zc} = (350.4 \pm 0.1)$ G. This value is however in perfect agreement with the previous determination by Feshbach spectroscopy [12].

In conclusion, we have detected and studied the role of the magnetic dipolar interaction (MDI) in a BEC-based atom interferometer. We have shown that MDI-induced decoherence can be suppressed by a proper choice of the scattering length. We have proved that the interferometer is sensitive to the MDI between different lattice sites. Our work constitutes a further step towards the realization of a high sensitivity interferometer employing a BEC with tunable interactions.

We acknowledge discussions with A. Simoni, M. Modugno, and the rest of the quantum gases group at LENS. This work was supported by MIUR (PRIN 2006), by EU(MEIF-CT-2004-009939), by INFN, and by Ente CRF, Firenze. B. D. acknowledges support under ESA contract SAI 20578/07/NL/UJ.

-
- [1] Y. Castin and J. Dalibard, Phys. Rev. A **55** 4330 (1997).
 [2] Y. Shin, *et al.*, Phys. Rev. Lett. **92** 050405 (2004).
 [3] G. B. Jo, *et al.*, Phys. Rev. Lett. **98**, 030407 (2007).
 [4] W. Li, *et al.*, Phys. Rev. Lett. **98** 040402 (2007).
 [5] M. Fattori, *et al.*, Phys. Rev. Lett. **100** 080405 (2008).
 [6] M. Gustavsson, E. Haller, M. J. Mark, J. G. Danzl, G. Rojas-Kopeinig, and H.-C. Nägerl, Phys. Rev. Lett. **100** 080404 (2008).
 [7] M. Fattori, T. Koch, S. Goetz, A. Griesmaier, S. Hensler, J. Stuhler, T. Pfau, Nature Phys. **2**, 765 (2006); T. Lahaye, T. Koch, B. Frhlich, M. Fattori, J. Metz, A. Griesmaier, S. Giovanazzi, T. Pfau, Nature **448**, 672 (2007).
 [8] M. Vengalattore, S. R. Leslie, J. Guzman, and D. M. Stamper-Kurn, Phys. Rev. Lett. **100**, 170403 (2008).
 [9] M. Dahan, E. Peik, J. Reichel, Y. Castin, and C. Salomon, Phys. Rev. Lett. **76**, 4508 (1996).
 [10] B. P. Anderson and M. A. Kasevich, Science **282**, 1686 (1998)
 [11] G. Roati, M. Zaccanti, C. D'Errico, J. Catani, M. Modugno, A. Simoni, M. Inguscio, and G. Modugno, Phys. Rev. Lett. **99**, 010403 (2007).
 [12] C. D'Errico, M. Zaccanti, M. Fattori, G. Roati, M. Inguscio, G. Modugno and A. Simoni, New. J. Phys. **9** 223 (2007).
 [13] D. Witthaut, M. Werder, S. Mossmann, and H. Korsch, Phys. Rev. E **71**, 036625 (2005).
 [14] Due to the hyperfine structure of ^{39}K , at 350 G the internal state of the atom in the $|I_z, S_z\rangle$ base, where I is the nuclear spin and S the electronic spin, is $|\psi\rangle = \alpha|3/2, -1/2\rangle + \beta|1/2, 1/2\rangle$ with $\alpha = -0.987305$ and $\beta = 0.158831$. This means that the effective magnetic dipole moment is $\langle \psi | \vec{\mu} | \psi \rangle = \langle \psi | -2\mu_B \vec{S} / \hbar | \psi \rangle = (\alpha^2 - \beta^2) \mu_B \hat{z} = 0.95 \mu_B \hat{z}$.
 [15] E. Demler, private communication.
 [16] L. Fallani, *et al.*, Phys. Rev. Lett. **93**, 140406 (2004)
 [17] S. Giovanazzi, A. Görlitz and T. Pfau, Phys. Rev. Lett. **89**, 130401 (2002).